Çukurova Üniversitesi
Mühendislik Fakültesi Dergisi
Çukurova University
Journal of the Faculty of Engineering
ISSN: 2757-9255 CİLT/VOLUME: 41 SAYI/ISSUE: 3 EYLÜL/SEPTEMBER 2026

Multi-Algorithm-Based Optimization of LQR Controller Parameters for a Triple Inverted Pendulum System

Berivan KOÇ [1,a], **Handan GÜRSOY-DEMİR** [2,b]

[1]*Iskenderun Technical University, Institute of Graduate Studies, Department of Computer Engineering, Hatay, Türkiye*
[2]*Iskenderun Technical University, Department of Computer Engineering, Hatay, Türkiye*

[a]***ORCID**: 0000-0003-0174-4872; [b]**ORCID**: 0000-0001-5486-454X*

Article Info
Received : 01.05.2026
Accepted : 08.09.2026
DOI: 10.21605/cukurovaumfd.1941490

Corresponding Author
Handan GÜRSOY-DEMİR
handan.gursoy@iste.edu.tr

Keywords
Triple inverted pendulum
LQR
Metaheuristic algorithms
Parameter optimization
Optimal control

***How to cite:** KOÇ, B., GÜRSOY-DEMİR, H., (2026). Multi-Algorithm-Based Optimization of LQR Controller Parameters for a Triple Inverted Pendulum System. Cukurova University, Journal of the Faculty of Engineering, 41(3), 663-678.*

ABSTRACT
This study addresses the Linear Quadratic Regulator (LQR)-based control of a triple inverted pendulum system with nonlinear, unstable, and multivariable dynamics. Since LQR performance depends on the selection of the Q and R weighting matrices, a total of nine parameters are optimized using metaheuristic algorithms. Genetic Algorithm (GA), Particle Swarm Optimization (PSO), Grey Wolf Optimization (GWO), Whale Optimization Algorithm (WOA), and Artificial Circulation System Algorithm (ACSA) are employed. The optimal LQR parameters obtained from each algorithm are compared under identical simulation conditions, and the performance is evaluated using ISE, ITAE, overshoot, settling time, and control effort. The results show that metaheuristic algorithms are effective in LQR parameter selection and improve the stabilization performance compared with the classical LQR controller. Among the investigated methods, ACSA-LQR achieves the best cart position performance, whereas GWO-LQR offers a favorable balance between control performance and convergence consistency.

Üçlü Ters Sarkaç Sistemi için LQR Denetleyici Parametrelerinin Çoklu Algoritma Tabanlı Optimizasyonu

Makale Bilgileri
Geliş : 01.05.2026
Kabul : 08.09.2026
DOI: 10.21605/cukurovaumfd.1941490

Sorumlu Yazar
Handan GÜRSOY-DEMİR
handan.gursoy@iste.edu.tr

Anahtar Kelimeler
Üçlü ters sarkaç
LQR
Meta-sezgisel algoritmalar
Parametre optimizasyonu
Optimal kontrol

***Atıf şekli:** KOÇ, B., GÜRSOY-DEMİR, H., (2026). Üçlü Ters Sarkaç Sistemi İçin LQR Denetleyici Parametrelerinin Çoklu Algoritma Tabanlı Optimizasyonu. Çukurova Üniversitesi, Mühendislik Fakültesi Dergisi, 41(3), 663-678.*

ÖZ
Bu çalışmada, doğrusal olmayan, kararsız ve çok değişkenli yapıya sahip üçlü ters sarkaç sisteminin Lineer Kuadratik Regülatör (LQR) tabanlı denetimi ele alınmıştır. LQR denetleyicinin başarımı Q ve R ağırlık matrislerinin seçimine bağlı olduğundan, dokuz parametre meta-sezgisel algoritmalarla optimize edilmiştir. Genetik Algoritma (GA), Parçacık Sürü Optimizasyonu (PSO), Gri Kurt Optimizasyonu (GWO), Balina Optimizasyon Algoritması (WOA) ve Yapay Dolaşım Sistemi Algoritması (ACSA) kullanılmıştır. Her bir algoritmadan elde edilen optimal LQR parametreleri aynı benzetim koşulları altında karşılaştırılmış ve denetleyici performansı ISE, ITAE, aşım, yerleşme süresi ve kontrol çabası ölçütleri kullanılarak değerlendirilmiştir. Sonuçlar, meta-sezgisel algoritmaların LQR parametre seçiminde etkili olduğunu ve dengeleme performansını klasik LQR'ye göre iyileştirdiğini göstermektedir. İncelenen yöntemler arasında ACSA-LQR araba konumu düzenlemesinde en başarılı sonuçları elde ederken, GWO-LQR kontrol performansı ve yakınsama tutarlılığı açısından daha dengeli bir çözüm sunmuştur.

1. INTRODUCTION

Inverted pendulum systems are among the most widely used benchmark problems in control theory due to their inherently unstable, nonlinear, and multivariable dynamics. These systems are extensively employed to evaluate the effectiveness of both classical and modern control methods, particularly because of their sensitivity around the equilibrium point and strict stability requirements [1-3].

Compared with single-link systems, multi-link inverted pendulum structures exhibit considerably more complex dynamics. These systems involve a high degree of nonlinearity, strong coupling among states, and increased system order. In this context, the triple inverted pendulum system stands out as a highly challenging control problem. The increase in system order strengthens the tendency toward instability and further complicates the control problem. Therefore, the triple inverted pendulum system is regarded as a critical platform for testing advanced and optimal control methods.

Among classical control methods, PID-based approaches are widely preferred due to their simple structure and ease of implementation. However, in multi-link and high-order nonlinear systems, they may be insufficient to provide the desired transient and steady-state performance. In such systems, state-feedback control structures offer more effective solutions. In this context, the Linear Quadratic Regulator (LQR), one of the fundamental methods of optimal control theory, stands out because it obtains the optimal control law by minimizing a quadratic cost function that considers both system performance and control effort.

The performance of the LQR controller directly depends on the proper selection of the weighting matrices Q and R. In the literature, these parameters are mostly determined using heuristic approaches or trial-and-error methods. However, this approach is time-consuming and, in most cases, produces non-optimal results. This issue becomes even more pronounced in high-dimensional systems such as the triple inverted pendulum, where parameter tuning turns into a complex optimization problem.

In the literature, LQR-based control approaches have been successfully applied to different inverted pendulum configurations. Early studies mostly focused on single-link systems and demonstrated the capability of the LQR method to balance the pendulum in the upright position [1,2]. With the transition to more complex systems, the LQR method has also been applied to double and triple inverted pendulum systems. For example, self-tuning LQR approaches have been developed for double inverted pendulum systems [4], while the stabilization of three-link systems has been addressed in various studies [5,6]. These studies show that, with appropriate parameter selection, LQR can also be an effective control method for high-order systems.

Nevertheless, the main issue in classical LQR design is the selection of the Q and R weighting matrices. Determining these matrices by trial and error in many studies may lead to non-optimal transient responses, high control effort, or weak robustness performance. Therefore, in recent years, metaheuristic algorithms have begun to be used for the systematic tuning of LQR weights. Önen et al. compared GA, PSO, and ABC algorithms for LQR controller design on a double inverted pendulum system; they derived the nonlinear model using the Lagrange method, linearized it around the equilibrium point, and tested different optimization structures [7]. Bilgiç et al. tuned the LQR weights using the Bees Algorithm on an experimental linear inverted pendulum setup and showed that the method could improve the pendulum angle and cart position responses on a real system [8].

GA- and PSO-based LQR optimization approaches have also been applied to rotary and double inverted pendulum systems, and it has been reported that they provide better transient performance and lower control effort compared with classical methods [9-11]. Xiong and Wan proposed a PSO-based LQR algorithm for a double inverted pendulum system, while Shen demonstrated the applicability of GA-based LQR design for a double inverted pendulum [10,11]. For three-link inverted pendulum systems, however, the literature is more limited, and GA-based LQR studies mostly come to the forefront. Shen performed LQR weighting matrix optimization using GA for a three-link inverted pendulum [12]. Abdullah et al. developed a Genetic LQR approach for a three-link inverted pendulum by defining the GA chromosome through the diagonal elements of the Q matrix and the R value [6].

Within the scope of more recent studies, it is observed that advanced metaheuristic algorithms such as Grey Wolf Optimization (GWO) have also been experimentally validated in LQR-based inverted pendulum

control [13]. However, when the literature is examined in general, it is noteworthy that the majority of studies focus on single or double pendulum systems or consider only a single optimization algorithm. Comprehensive studies in which multiple metaheuristic algorithms are compared under the same conditions on the same triple inverted pendulum model appear to be limited.

Motivated by this literature gap, this study proposes an LQR-based control structure for the triple inverted pendulum system and optimizes the weighting matrices using different metaheuristic algorithms. In this context, in addition to GA, PSO, GWO, and the Whale Optimization Algorithm (WOA), the Artificial Circulation System Algorithm (ACSA), which effectively provides an exploration–exploitation balance and is relatively new in the literature, is also evaluated. An optimization problem consisting of nine parameters is considered, including eight Q weighting coefficients and one scalar R control weight and the performance of the algorithms is comparatively analyzed in terms of time-domain criteria, error indices, and control signal behavior.

The principal contribution of this study lies in establishing a unified framework for the metaheuristic tuning of the LQR weighting parameters of a triple inverted pendulum system. In contrast to approaches that focus on a single algorithm or optimize only a restricted subset of controller parameters, all eight diagonal elements of the (Q) matrix and the scalar (R) parameter are simultaneously determined using GA, PSO, GWO, WOA, and ACSA under identical computational conditions. Furthermore, to the best of the authors' knowledge, this study is the first to investigate ACSA for LQR weighting parameter optimization in an inverted pendulum system. The resulting controllers are assessed through error indices, transient-response characteristics, control effort, actuator demand, convergence behavior, and variability across independent runs. This framework enables a consistent evaluation of both optimization efficiency and closed-loop control performance, thereby providing a broader basis for selecting suitable LQR parameters for highly coupled and high-order unstable systems.

The remainder of the paper is organized as follows: Section 2 presents the mathematical model and state-space representation of the triple inverted pendulum system. Section 3 discusses the LQR controller design and the effects of weighting matrices on system performance. Section 4 explains the metaheuristic optimization algorithms used in the study. Section 5 presents the simulation results and comparatively analyzes the methods. Finally, Section 6 summarizes the study and discusses possible future work.

2. MATHEMATICAL MODEL OF THE PLANT

The triple inverted pendulum system is a high-order, nonlinear, and inherently unstable mechanical system consisting of three pendulum elements connected in series on a cart capable of linear motion. The system is defined by the cart position, pendulum angles, and their corresponding velocity components. Due to the multi-pendulum structure, the system dynamics exhibit a complex behavior involving mass interactions, angular coupling, gravitational effects, moments of inertia, and damping terms. Therefore, the triple inverted pendulum system is considered a highly challenging benchmark system for testing advanced control methods.

In this study, the mathematical model of the triple inverted pendulum system is derived using generalized coordinates. The generalized coordinate vector of the system is defined in Equation 1:

$$q = [x\ \alpha\ \beta\ \gamma]^T \tag{1}$$

Here, x represents the linear position of the cart, while α, β, and γ denote the angular displacements of the first, second, and third pendulums, respectively. The velocity vector corresponding to these variables is given in Equation 2,

$$\dot{q} = \left[\dot{x}\ \dot{\alpha}\ \dot{\beta}\ \dot{\gamma}\right]^T \tag{2}$$

The equations of motion of the triple inverted pendulum system can be expressed in a compact matrix form in terms of generalized coordinates as given in Equation 3:

$$M(q)\ddot{q} = F(q, \dot{q}, u) \tag{3}$$

Here, $M(q)$ represents the position-dependent mass/inertia matrix of the system, while $F(q,\dot{q},u)$ denotes the nonlinear force/moment vector that includes the effects of gravity, centrifugal forces, Coriolis terms, damping, and control input. This vector can be generally expressed as (Equation 4).

$$F(q,\dot{q},u) = \tau - C(q,\dot{q}) - G(q) - D\dot{q} \tag{4}$$

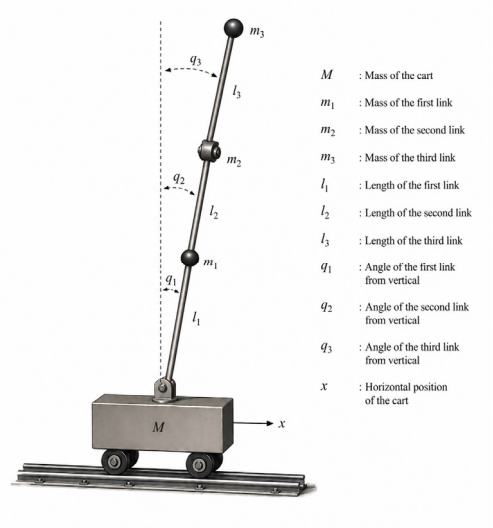


Figure 1. Triple inverted pendulum

Here, τ represents the input force applied to the system; $C(q,\dot{q})$ denotes the centrifugal and Coriolis effects; $G(q)$ represents the gravity-induced terms; and $D\dot{q}$ expresses the linear and angular damping effects. The trigonometric terms present in the elements of the mass matrix indicate the angular coupling between the pendulums, while the velocity-dependent terms in the force vector reveal the nonlinear dynamic characteristics of the system. In the triple inverted pendulum system, the control input is only the horizontal force applied to the cart. Therefore, the input vector is expressed as given in Equation 5.

$$\tau = [u\ 0\ 0\ 0]^T \tag{5}$$

Accordingly, the control input directly affects the linear motion of the cart; however, due to the dynamic coupling between the pendulums, it creates an indirect effect on all angular variables. This situation is one of the main factors that makes the control of the triple inverted pendulum system challenging. The nonlinear acceleration vector is obtained as given in Equation 6:

$$\ddot{q} = M^{-1}(q)F(q,\dot{q},u) \tag{6}$$

This equation constitutes the fundamental nonlinear dynamic model used in numerical simulations and the linearization process.

The physical parameters of the triple inverted pendulum system used in this study are given in Table 1. The parameters consist of the cart mass, pendulum masses, pendulum lengths, moments of inertia, damping coefficients, and gravitational acceleration.

Table 1. Mechanical parameters of the triple inverted pendulum on a cart

Parameter	Cart (i=0)	Arm-1 (i=1)	Arm-2 (i=2)	Arm-3 (i=3)	Unit
Mass (m_i)	0.969	0.204	0.150	0.070	kg
Length (L_i)	–	0.25	0.20	0.15	m
Moment of inertia (I_i)	–	0.001688	0.001100	0.000300	kg·m²
Cart damping d_0	0.5	–	–	–	N·s/m
Damping coefficient (d_i)	–	0.01	0.01	0.01	N·m·s/rad

This mathematical modeling approach enables the nonlinear and highly coupled dynamics of the system to be represented in a compact form. The obtained model both describes the physical behavior of the system and provides a basis for LQR controller design through linearization.

3. LQR CONTROLLER DESIGN

The Linear Quadratic Regulator (LQR) is one of the optimal control methods based on state feedback [8]. The main objective of this method is to minimize a performance index that simultaneously considers the deviation of the system states from the equilibrium point and the magnitude of the control signal. Therefore, the LQR approach provides a balanced controller design in terms of both stability and control energy.

Since the triple inverted pendulum system has a high-order, coupled, and unstable structure, it is difficult to achieve the desired performance using classical control methods based only on output error. In contrast, the LQR controller incorporates all system state variables into the feedback structure and provides simultaneous control over the cart position, pendulum angles, and their corresponding velocity components. This feature makes the LQR method a strong controller candidate for multivariable systems such as the triple inverted pendulum.

The linearized system model is expressed in the state-space form given in Equation 7 as follows:

$$\dot{X} = AX + Bu \tag{7}$$

Here, X denotes the system state vector, u denotes the control input, A denotes the system matrix, and B denotes the input matrix. In this study, the state vector is defined as follows (Equation 8):

$$X = [x \quad \dot{x} \quad \alpha \quad \dot{\alpha} \quad \beta \quad \dot{\beta} \quad \gamma \quad \dot{\gamma}] \tag{8}$$

The control law in the LQR controller is expressed as given in Equation 9:

$$u(t) = -KX(t) \tag{9}$$

Here, K is the LQR feedback gain matrix. This gain matrix is calculated to minimize the selected performance index. The performance index used in the LQR method is given in Equation 10 as follows:

$$J = \int_0^\infty (X^T QX + u^T Ru)dt \tag{10}$$

In this expression, the Q matrix represents the weights assigned to the system states, while the R matrix represents the weight assigned to the control input. Larger values in the Q matrix provide stricter control of the corresponding state variable, whereas increasing the R value limits the magnitude of the control signal. Therefore, the selection of the Q and R matrices has a direct effect on the system response.

In this study, the Q matrix is selected in diagonal form and defined by eight weighting coefficients corresponding to the eight state variables (Equation 11):

$$Q = \text{diag}(q_1, q_2, q_3, q_4, q_5, q_6, q_7, q_8) \tag{11}$$

Here, q_1 denotes the weighting coefficient for the cart position, q_2 for the cart velocity, q_3 for the first pendulum angle, q_4 for the angular velocity of the first pendulum, q_5 for the second pendulum angle, q_6 for the angular velocity of the second pendulum, q_7 for the third pendulum angle, and q_8 for the angular velocity of the third pendulum.

The control weight is defined as a scalar (Equation 12):

$$R = r \tag{12}$$

The LQR gain is obtained by solving the continuous-time algebraic Riccati equation, as given in Equation 13:

$$A^T P + PA - PBR^{-1}B^T P + Q = 0 \tag{13}$$

Here, P is the symmetric positive-definite Riccati solution matrix. After this matrix is obtained, the feedback gain is calculated as follows (Equation 14):

$$K = R^{-1}B^T P \tag{14}$$

Thus, the closed-loop system dynamics are expressed as follows (Equation 15):

$$\dot{X} = (A - BK)X \tag{15}$$

The stability of the closed-loop system depends on the eigenvalues of the $(A - BK)$ matrix being located in the left half-plane. Therefore, the appropriate selection of Q and R directly affects not only the transient response performance but also the closed-loop stability.

In this study, the main parameters to be optimized for the LQR controller are the diagonal elements of the Q matrix and the scalar R control weight. Thus, the controller design is considered as a nine-dimensional parameter optimization problem, consisting of eight Q weights and one R weight. Instead of the classical trial-and-error approach, these weighting coefficients are determined using metaheuristic algorithms. In this way, it is aimed to improve the stabilization performance of the triple inverted pendulum system, enhance time-domain criteria such as overshoot and settling time, and obtain a more balanced control signal.

4. METAHEURISTIC OPTIMIZATION-BASED LQR PARAMETER TUNING

4.1. Definition of the Optimization Problem

The performance of the LQR controller directly depends on the appropriate selection of the Q and R weighting matrices. However, especially in high-order, coupled, and unstable systems such as the triple inverted pendulum, determining these weights by trial and error is both time-consuming and heuristic. Therefore, in this study, the diagonal elements of the Q matrix and the scalar R control weight of the LQR controller are determined using metaheuristic optimization algorithms.

In this context, each candidate solution is defined as a nine-dimensional parameter vector in Equation 16:

$$z = [q_1, q_2, q_3, q_4, q_5, q_6, q_7, q_8, r],\ R = r \tag{16}$$

Each q_i value in this vector represents the corresponding diagonal element of the Q matrix used in the LQR controller, and r denotes the scalar control weight of the R matrix (Equation 17):

$$Q = \text{diag}(q_1, q_2, q_3, q_4, q_5, q_6, q_7, q_8) \tag{17}$$

During the optimization process, for each candidate solution, the Q matrix was first constructed, then the LQR gain matrix K was calculated, and the time response of the triple inverted pendulum system was obtained. The objective function defined based on the obtained system response was then computed, and the algorithms were executed to minimize this value.

As seen in Table 2, the optimization problem includes the simultaneous determination of both the weights assigned to the state variables and the weight assigned to the control input. Through this structure, the LQR design aims not only to reduce state errors but also to regulate the control effort in a balanced manner. Running all algorithms under the same bounds and operating conditions enables a fair comparison of the obtained results.

Table 2. Parameters and search bounds used in LQR optimization

Parameter	Value
Optimization dimension	9 (8Q + 1R)
Optimized parameters	*q1, q2, q3, q4, q5, q6, q7, q8, r*
Lower bound	[1, 10, 10, 10, 1, 1, 1, 1, 0.1]
Upper bound	[500, 2000, 1500, 1000, 300, 300, 300, 300, 100]
Simulation time	10 s
Time step	0.01 s
Population size	25
Number of iterations	50
Number of runs	20

In addition to the common optimization settings presented in Table 2, each metaheuristic algorithm was implemented using its own characteristic control parameters. The initial candidate solutions were generated using a uniform random distribution within the specified search bounds. Candidate solutions exceeding the allowable limits during the update process were restricted to the corresponding lower or upper bounds. The algorithm-specific parameter settings used in the implementation are summarized in Table 3.

Table 3. Algorithm-specific parameter settings used in the optimization process

Algorithm	Algorithm-specific parameter settings
GA	Roulette-wheel selection; selection pressure ($\boldsymbol{\beta = 8}$); arithmetic crossover; crossover probability ($\boldsymbol{p_c = 0.8}$); mutation probability ($\boldsymbol{p_m = 0.3}$); mutation rate ($\boldsymbol{\mu = 0.1}$); Gaussian mutation standard deviation ($\boldsymbol{\sigma = 0.1}$(UB − LB))
PSO	Initial inertia weight ($\boldsymbol{w = 0.7}$); inertia damping coefficient ($\boldsymbol{w}_{\text{damp}} \boldsymbol{= 0.99}$); cognitive coefficient ($\boldsymbol{c_1 = 1.5}$); social coefficient ($\boldsymbol{c_2 = 1.5}$); maximum velocity ($\boldsymbol{V_{max} = 0.2}$(UB − LB))
GWO	Control parameter (*a*) linearly decreased from 2 to 0; random coefficients ($\boldsymbol{r_1, r_2} \in \boldsymbol{[0, 1]}$); search process guided by the ($\boldsymbol{\alpha}$), ($\boldsymbol{\beta}$), and ($\boldsymbol{\delta}$) wolves
WOA	Control parameter (*a*) linearly decreased from 2 to 0; auxiliary parameter ($\boldsymbol{a_2}$) decreased from (-1) to (-2); spiral constant ($\boldsymbol{b = 1}$); switching probability ($\boldsymbol{p = 0.5}$)
ACSA	Neural regulator ratio ($\boldsymbol{NH}_{\text{rate}} \boldsymbol{= 0.10}$); step factor ($\boldsymbol{S = 0.01}$); neural coefficients ($\boldsymbol{E_{a,n} = 1.8}$) and ($\boldsymbol{E_{s,n} = 0.002}$); hormonal coefficients ($\boldsymbol{E_{a,h} = 0.66}$) and ($\boldsymbol{E_{s,h} = 0.33}$)

4.2. Genetic Algorithm (GA)

Genetic Algorithm is a population-based optimization method inspired by natural selection and genetic inheritance mechanisms [14-15]. In the algorithm, each individual represents a candidate solution. In this study, each individual consists of the eight *Q* weighting coefficients and the scalar *R* control weight of the LQR controller.

In GA, the initial population is generated randomly, and the fitness value of each individual is calculated using the objective function. Then, selection, crossover, and mutation operations are applied to generate new individuals. The selection process increases the probability of transferring more successful individuals to the next generation, while crossover enables information exchange between existing good solutions. Mutation preserves diversity in the solution space and reduces the risk of the algorithm becoming trapped in a local optimum.

4.3. Particle Swarm Optimization (PSO)

Particle Swarm Optimization is a population-based optimization algorithm inspired by the collective movement behavior of bird flocks and fish schools [16-17]. In PSO, each particle represents a candidate solution in the search space, and the position of the particle corresponds to the parameter vector being optimized. In this study, the particle position z consists of the LQR weighting coefficients.

Each particle is updated by considering its own best position found so far and the best position found by the entire swarm. The velocity and position update equations of PSO are given in Equations 18-19 as follows:

$$v_i^{k+1} = wv_i^k + c_1 r_1 \left(p_i^k - z_i^k\right) + c_2 r_2 \left(g^k - z_i^k\right) \tag{18}$$

$$z_i^{k+1} = z_i^k + v_i^{k+1} \tag{19}$$

Here, $\boldsymbol{v_i}$ denotes the particle velocity, $\boldsymbol{z_i}$ denotes the particle position, $\boldsymbol{p_i}$ denotes the personal best position of the particle, and $\boldsymbol{g}$ denotes the global best position of the swarm. The parameter w is the inertia weight, c1 and c2 are the cognitive and social learning coefficients, and r1 and r2 are random numbers in the range [0,1].

4.4. Grey Wolf Optimization (GWO)

Grey Wolf Optimization is a metaheuristic optimization algorithm inspired by the social hierarchy and hunting strategy of grey wolves [18]. In the algorithm, the best solution is denoted as α, the second-best solution as β, the third-best solution as δ, and the remaining candidate solutions as ω. The search process is guided by the α, β, and δ solutions. In the original GWO study, this hierarchical structure and the encircling/attacking behaviors are modeled as the main search mechanisms [18-19].

In GWO, the encircling behavior is expressed by Equations 20-21 as follows:

$$D = \left|C \cdot X_p(k) - X(k)\right| \tag{20}$$

$$X(k+1) = X_p(k) - A \cdot D \tag{21}$$

Since the exact position of the prey is unknown, the three best candidate solutions, α, β, and δ, are assumed to guide the search process. Accordingly, the distance vectors between a search agent and the leading wolves are calculated as

$$D_j = \left|C_j \cdot X_j - X\right|, \quad j \in \{\alpha, \beta, \delta\} \tag{22}$$

Then, the candidate positions guided by each leading wolf are obtained using Equation (23).

$$X_j' = X_j - A_j \cdot D_j, \quad j \in \{\alpha, \beta, \delta\} \tag{23}$$

Finally, the updated position of each search agent is calculated by averaging these three candidate positions, as given in Equation (24).

$$X(k+1) = \frac{X_\alpha' + X_\beta' + X_\delta'}{3} \tag{24}$$

In this study, each grey wolf represents a candidate LQR parameter vector. Therefore, the position vector X is defined in Equation (25).

$$X = [q_1, q_2, q_3, q_4, q_5, q_6, q_7, q_8, r] \tag{25}$$

where q1–q8 are the diagonal elements of the Q weighting matrix and r is the scalar control weighting parameter. During the optimization process, each candidate vector is evaluated using the objective function defined for the closed-loop triple inverted pendulum system, and the best parameter set is selected according to the minimum cost value.

4.5. Whale Optimization Algorithm (WOA)

The Whale Optimization Algorithm is inspired by the hunting behavior of humpback whales, particularly the spiral hunting strategy known as the bubble-net method [20]. In WOA, candidate solutions represent whales, while the best solution represents the position of the prey. The algorithm performs the search in the solution space using encircling, spiral updating, and random search mechanisms. In the original WOA study, the algorithm was tested on mathematical benchmark problems and engineering design problems.

The encircling behavior is expressed by Equations 26-27 as follows:

$$D = \left|C \cdot X_p(k) - X(k)\right| \tag{26}$$

$$X(k+1) = X_p(k) - A \cdot D \tag{27}$$

Here, X_p represents the position of the prey or the best solution obtained so far, and X represents the current position of a whale. The coefficient vectors A and C are defined as follows (Equations 28-29):

$$A = 2ar_1 - a \tag{28}$$

$$C = 2r_2 \tag{29}$$

Here, the coefficient a is linearly decreased from 2 to 0 over the course of iterations, while r_1 and r_2 are random vectors in the range [0,1]. In this study, the vector X corresponds to the vector z containing the LQR weighting coefficients.

In addition to the encircling mechanism given in Equations (26)–(29), WOA also models the bubble-net attacking behavior of humpback whales using a spiral updating strategy. In this mechanism, the distance between the current whale and the best solution is calculated using Equation (30).

$$D' = \left|X_p(k) - X(k)\right| \tag{30}$$

Then, the spiral position update is performed according to Equation (31).

$$X(k+1) = D' \cdot e^{bl} \cdot \cos(2\pi l) + X_p(k) \tag{31}$$

where b is a constant defining the shape of the logarithmic spiral, and l is a random number in the interval $[-1,1]$. During the optimization process, WOA switches between the encircling and spiral updating mechanisms according to a probability value p. In addition, when $|A| \geq 1$, the algorithm performs a random search around a randomly selected whale to enhance exploration. In this study, each whale represents a candidate LQR parameter vector z containing the eight Q weighting coefficients and the scalar R control weight.

4.6. Artificial Circulation System Algorithm (ACSA)

The Artificial Circulation System Algorithm is a new-generation metaheuristic optimization algorithm inspired by the biological circulatory system and its hormonal/neural regulation mechanisms [21]. ACSA employs a population-based search strategy and updates the positions of candidate solutions using a distinctive update mechanism. In the literature, the algorithm has been reported to provide competitive results in terms of global search, local search, and exploration–exploitation balance [21,22].

In this study, ACSA is used to determine the LQR weighting coefficients. Each candidate solution is considered as an individual/agent in the circulatory system, and each agent is represented by an eight-dimensional Q weighting vector and the scalar R control weight. The use of ACSA in this study is important for evaluating the performance of a new-generation optimization algorithm on a highly unstable control problem such as the triple inverted pendulum. To the best of the authors' knowledge, ACSA has not previously been investigated for LQR weight optimization in inverted pendulum systems. Therefore, its application to the triple inverted pendulum system constitutes one of the novel aspects of this study.

The general candidate solution structure for ACSA is given in Equation 32:

$$X_i = [x_{i,1}, x_{i,2}, \dots, x_{i,D}], \qquad D = 9 \tag{32}$$

In this study, $D=9$, where the first eight dimensions correspond to the diagonal elements of the LQR Q matrix, and the ninth dimension corresponds to the scalar R control weight.

4.7. Objective Function and Performance Metrics

For a fair comparison of the optimization algorithms, the same objective function and performance metrics were used for all methods. Thus, the effectiveness of GA, PSO, GWO, WOA, and ACSA in determining the LQR parameters was evaluated under consistent and comparable conditions.

The objective function was defined to simultaneously consider the cart position error, pendulum angle errors, control energy, maximum angular deviation, settling time, and steady-state errors. In this way, the optimization process was directed not only toward reducing error values but also toward obtaining LQR parameters that yield low oscillation, fast settling, and reasonable control effort.

$$J = w_1 J_x + w_2 J_\theta + w_3 J_u + w_4 OS_\theta + w_5 T_s + w_6 E_x + w_7 E_\theta \tag{33}$$

Here, J_x denotes the integral of squared cart position error, J_θ represents the total squared error integral of the three pendulum angles, J_u denotes the squared integral of the control force, OS_θ is the total maximum angular deviation, T_s is the total settling time, E_x is the final cart position error, and E_θ is the final total angular error. The terms OS_θ and E_θ were calculated in degrees, and w_i represents the weighting coefficients used in the objective function.

In this study, the weighting coefficients were selected as $w_1 = 80,\ w_2 = 150,\ w_3 = 0.06,\ w_4 = 35,\ w_5 = 35,\ w_6 = 150, and\ w_7 = 25$. These coefficients were determined through preliminary simulation studies and trial-and-error analyses to balance the contributions of the objective-function terms with different numerical scales. Higher weights were assigned to the cart position error, pendulum angle error, and final cart position error to prioritize stabilization and position regulation, whereas a relatively small coefficient was assigned to the control-energy term to prevent it from dominating the objective function. The same weighting coefficients were used for all optimization algorithms to ensure a fair comparison.

In addition to the objective function used during optimization, several time-domain performance metrics were calculated to evaluate the closed-loop responses of the controllers. The Integral of Squared Error (ISE) measures the accumulated squared error over the simulation period and gives greater emphasis to large deviations. For a given error signal $e(t)$, ISE is defined as

$$ISE = \int_0^T e^2(t)\ dt \tag{34}$$

The Integral of Time-weighted Absolute Error (ITAE) penalizes errors that persist for a longer time and is therefore useful for evaluating the settling behavior of the system. ITAE is expressed by Equation (35) as follows:

$$ITAE = \int_0^T t|e(t)|\ dt \tag{35}$$

In addition to ISE and ITAE, the maximum absolute cart displacement, maximum control input, root-mean-square control input, and control energy were also considered. These metrics are given as (Equations 36-39)

$$Max.|x| = max\,|x(t)| \tag{36}$$

$$Umax = max\,|u(t)| \tag{37}$$

$$u_{RMS} = \sqrt{\frac{1}{T}\int_0^T u^2(t)\ dt} \tag{38}$$

$$E_u = \int_0^T u^2(t)\ dt \tag{39}$$

where $x(t)$ is the cart position, $u(t)$ is the control input, and T is the total simulation time. These metrics enable the controllers to be evaluated not only in terms of cart position regulation and angular stabilization, but also with respect to control effort and actuator requirements.

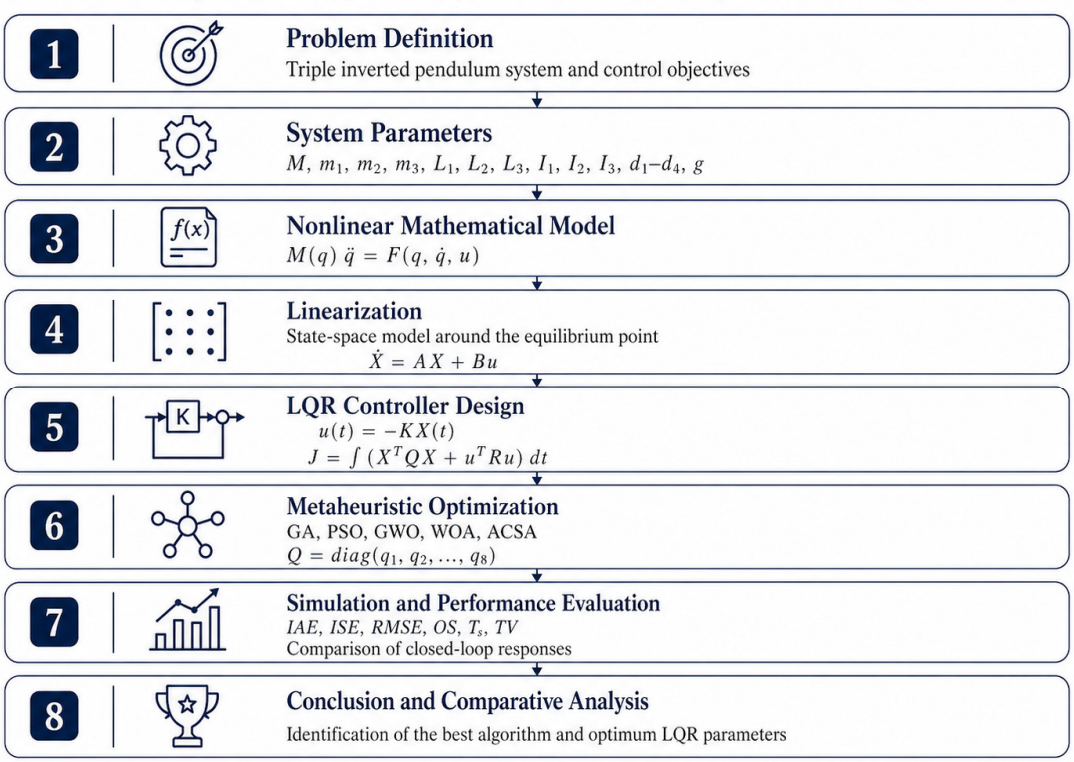


Figure 2. General workflow of the proposed LQR–MHA-based controller design

The overall workflow of the proposed LQR–MHA-based controller design is illustrated in Figure 2. As shown in the figure, the study consists of nonlinear modeling, linearization, LQR controller design, metaheuristic optimization, and performance evaluation stages.

5. SIMULATION RESULTS AND COMPARATIVE ANALYSIS

In this section, the closed-loop performances of classical LQR, GA-LQR, PSO-LQR, GWO-LQR, WOA-LQR, and ACSA-LQR controllers on the triple inverted pendulum system are compared. All simulations were carried out under identical initial conditions, system parameters, and simulation duration. The performance of the controllers was evaluated based on the responses of the three pendulum angles, cart position, and control force, while the numerical comparison was supported by performance metrics such as ISE, ITAE, maximum deviation, and control energy.

The cart position response presented in Figure 3 shows that the metaheuristic-optimized LQR controllers improve the transient behavior of the system compared with the classical LQR. The classical LQR exhibits a larger cart displacement and a slower return toward the equilibrium position. In contrast, the GA-LQR, PSO-LQR, GWO-LQR, WOA-LQR, and ACSA-LQR controllers reduce the cart displacement and provide a faster recovery. The responses of the optimized controllers are generally close to each other, with ACSA-LQR exhibiting the most favorable cart position response and the remaining optimized responses showing generally close behavior. Although a small positive overshoot is observed after the initial recovery, all optimized controllers converge smoothly to the equilibrium position without noticeable oscillations. Overall, the results indicate that optimizing the LQR weighting matrices improves cart position regulation and enhances the transient response of the system.

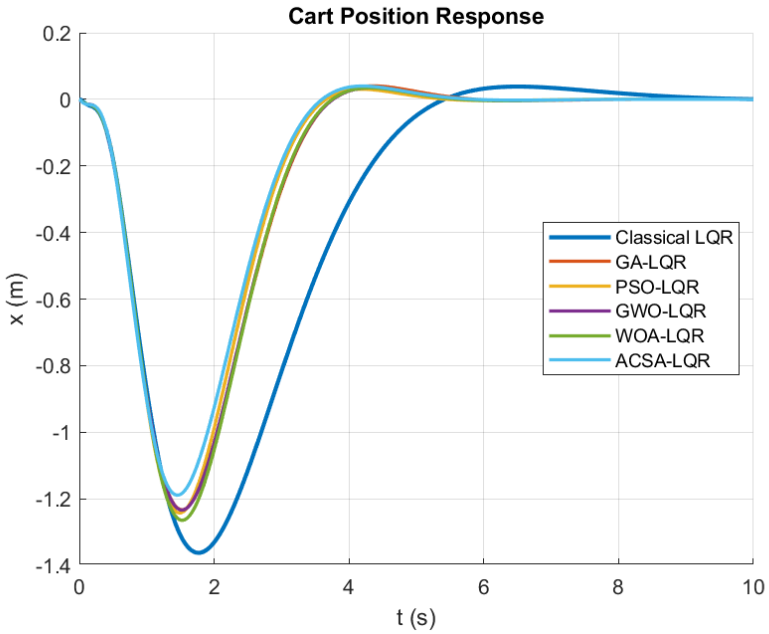


Figure 3. Cart position response

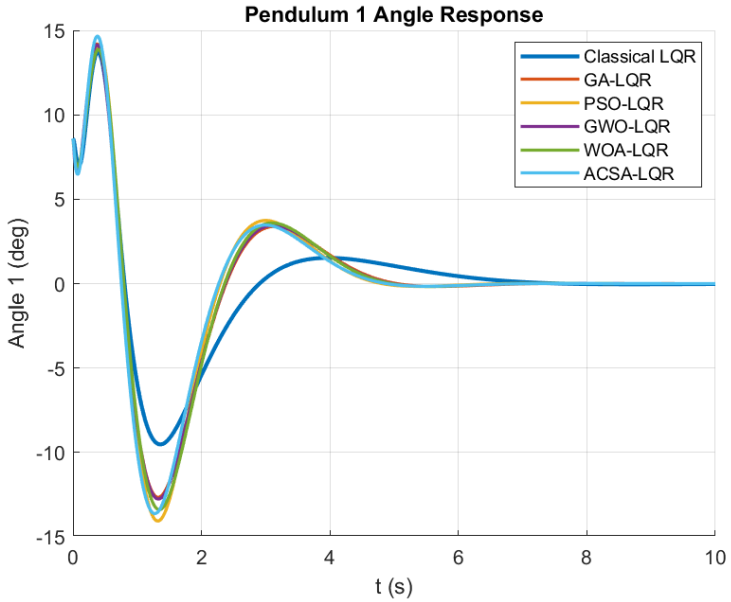


Figure 4. First pendulum angle response

As shown in Figure 4, all controllers successfully stabilize the first pendulum angle around the equilibrium position. The classical LQR exhibits a smoother but slower response, whereas the optimized LQR controllers provide faster convergence. Although GA-LQR, PSO-LQR, GWO-LQR, WOA-LQR, and ACSA-LQR produce slightly larger initial angular oscillations, their responses settle more rapidly. Overall, the optimized controllers improve the convergence speed while maintaining stable angle regulation.

The second and third pendulum angle responses are shown in Figure 5. In both cases, all controllers successfully stabilize the system around the equilibrium position. The optimized LQR controllers generally provide faster damping and shorter settling times compared with the classical LQR. Although minor differences are observed in the initial oscillations, all responses decay smoothly and remain within a limited angular range. Overall, the results indicate that metaheuristic-based LQR tuning improves the convergence characteristics of the second and third pendulum angles.

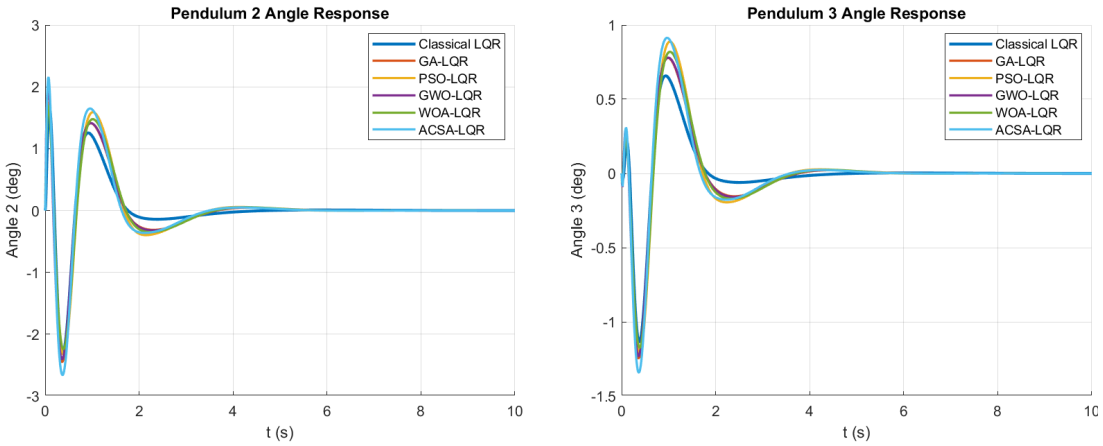


Figure 5. Responses of the second and third pendulum angles

Figure 6 presents the control input responses of the classical and optimized LQR controllers. All controllers generate a relatively high control action at the initial instant, followed by a rapidly damped force response that converges toward zero. The optimized LQR controllers exhibit slightly higher transient control amplitudes than the classical LQR, which is consistent with their faster stabilization behavior observed in the state responses. However, after the initial transient phase, all control signals remain smooth and settle without sustained oscillations. Overall, the results indicate that the metaheuristic-optimized LQR controllers achieve improved transient performance at the expense of a moderately increased initial control action.

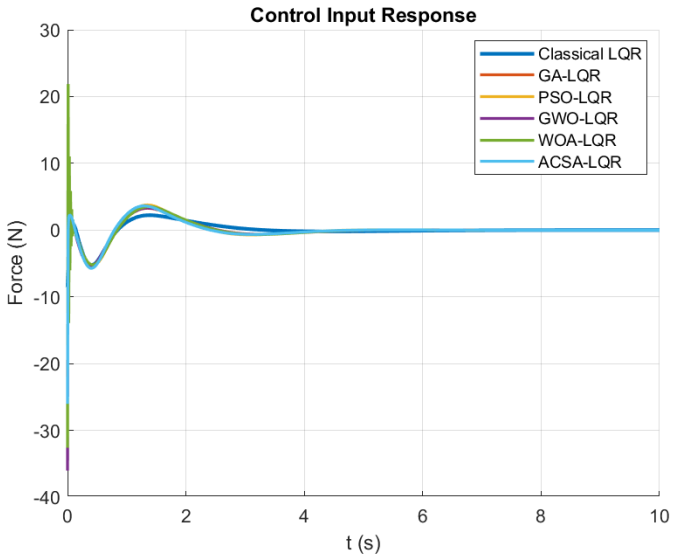


Figure 6. Control force response

The convergence curves in Figure 7 show the optimization behavior of GA, PSO, GWO, WOA, and ACSA over 20 independent runs. In the individual run plots, GA, PSO, GWO, and WOA generally exhibit a decreasing cost trend, indicating progressive improvement of the LQR weighting parameters during the optimization process. GWO exhibits relatively fast convergence and closely clustered final cost values, indicating more consistent performance across the independent runs. WOA also converges rapidly, although its final solutions show greater run-to-run variation. GA and PSO exhibit comparatively higher variability, while GA generally requires more iterations to approach its final cost level. ACSA reaches stable cost values within the early iterations; however, the considerable dispersion among its individual runs suggests greater sensitivity to the initial search conditions. The mean convergence curves show that WOA, PSO, and GWO achieve lower average final cost values, whereas GA converges more gradually and ACSA exhibits limited average improvement after the initial iterations.

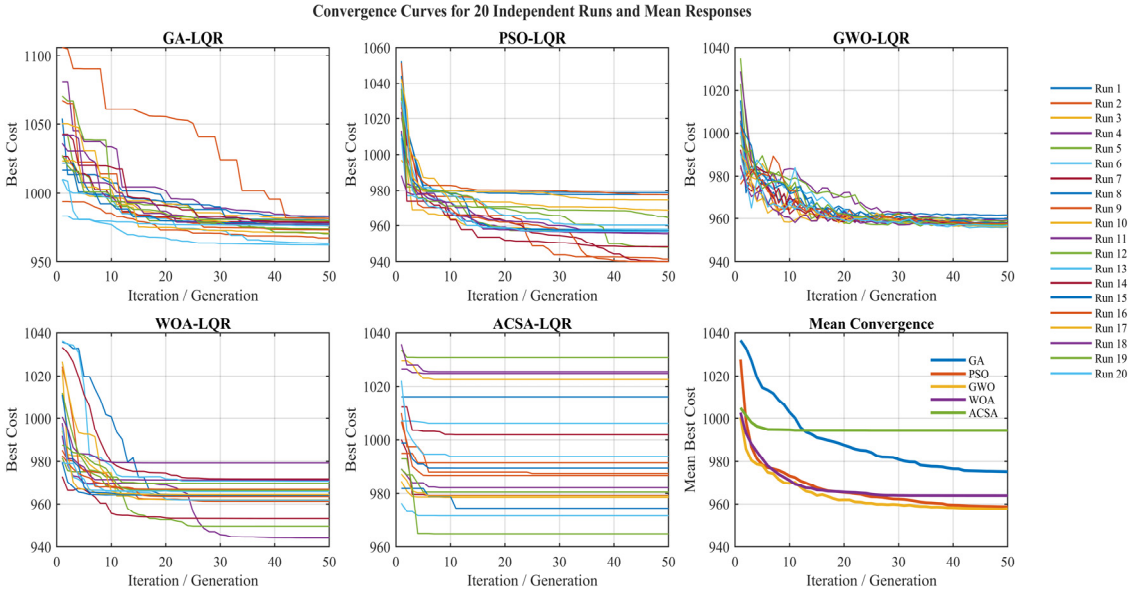


Figure 7. Convergence behavior of the metaheuristic algorithms over 20 independent runs and mean convergence responses

The main performance metrics of the controllers are presented in Table 4. The results demonstrate that metaheuristic-based optimization substantially enhances the cart position regulation performance of the LQR controller. Among all methods, ACSA-LQR achieves the lowest ISE_x, $ITAE_x$, and maximum absolute cart displacement, indicating the most effective cart position response. PSO-LQR also provides strong position regulation performance, while GA-LQR and GWO-LQR achieve competitive results across the evaluated position metrics. These improvements are accompanied by moderate increases in angular error and control effort, reflecting the expected trade-off between faster position recovery and control action. Among the optimized controllers, GA-LQR requires the lowest peak control input, RMS control input, and control energy, thereby offering an efficient balance between position regulation and control effort. Overall, the results confirm the effectiveness of metaheuristic optimization in improving LQR performance. ACSA-LQR provides the best cart position regulation, while GWO-LQR offers a competitive overall performance by achieving favorable position control with moderate control effort. GA-LQR, on the other hand, requires the lowest control effort among the optimized controllers.

Table 4. Performance comparison of classical LQR and metaheuristic-optimized LQR controllers

Controller	ISE_x	ISE0	$ITAE_x$	Max. |x|	Max. |u|	u_{RMS}	E_u
Classical LQR	3.3022	0.0482	8.0585	1.3624	8.5204	1.1980	14.0029
GA-LQR	1.9462	0.0635	3.9825	1.2330	22.3684	1.5144	20.4541
PSO-LQR	1.8607	0.0699	3.6317	1.2425	32.2746	1.9015	30.9848
GWO-LQR	1.9382	0.0639	3.9175	1.2340	36.0235	1.8277	26.9491
WOA-LQR	2.0061	0.0671	3.9592	1.2646	32.6038	1.9377	32.2693
ACSA-LQR	1.7097	0.0672	3.5088	1.1891	26.0289	1.6184	22.8301

Overall, the results demonstrate that metaheuristic-based optimization of the LQR weighting matrices improves the closed-loop performance of the triple inverted pendulum system, particularly in terms of cart position regulation. ACSA-LQR achieves the best cart position performance by providing the lowest ISE_x, $ITAE_x$, and maximum displacement values. However, the convergence analysis shows that ACSA exhibits considerable run-to-run variability, whereas GWO provides the most consistent optimization behavior and PSO and WOA show moderate repeatability. Therefore, ACSA-LQR should be interpreted as the most effective controller with respect to the evaluated closed-loop performance metrics, rather than as the most robust optimization method in terms of convergence consistency. These findings highlight the importance of evaluating controller performance together with optimization repeatability, angular response, control effort, and actuator limitations.

6. CONCLUSIONS

In this study, classical LQR and metaheuristic-optimized LQR approaches were comparatively investigated for the control of the triple inverted pendulum system. The simulation results show that optimizing the LQR weighting matrices substantially improves the closed-loop performance compared with the classical LQR. All optimized controllers reduce the cart position error and provide faster transient responses.

Among the optimized methods, ACSA-LQR achieves the best overall cart position regulation performance, with the lowest ISE_x, $ITAE_x$, and maximum absolute cart displacement values. This improvement is accompanied by increased angular error and control effort compared with the classical LQR, reflecting the trade-off between faster cart position recovery and control action. GWO-LQR provides a favorable overall balance between control performance and convergence consistency, while GA-LQR requires the lowest control effort among the optimized controllers. The convergence results further show that controller selection should not be based solely on the best final solution, since ACSA exhibits greater run-to-run variability, whereas GWO, WOA, and PSO demonstrate more consistent convergence trends.

Overall, the results indicate that metaheuristic-based tuning of LQR weighting matrices provides a systematic and effective alternative to trial-and-error-based LQR design. Nevertheless, the selection of the most suitable controller should consider position error, angular response, control effort, convergence consistency, and actuator requirements together. In this context, the proposed optimization-based LQR framework can be considered a practical and extensible approach for the control of high-order unstable systems such as the triple inverted pendulum.

7. ACKNOWLEDGMENT

This study was derived from the first author's master's thesis.

Declaration of generative AI and AI-assisted technologies in the manuscript preparation process

During the preparation of this work, the authors used ChatGPT solely for language editing and to improve readability and clarity. All scientific content, methodology, analyses, results, and conclusions were developed and verified by the authors, who take full responsibility for the final content of the published article.

8. REFERENCES

1. Wan, L.L., Lei, J. & Wu, H.X. (2014). Design of LQR controller for the inverted pendulum. *Advanced Materials Research, 1037*, 221-224.
2. Shehu, M.A., Ahmad, M.R., Shehu, A. & Alhassan, A.B. (2015). LQR, double-PID and pole placement stabilization and tracking control of single link inverted pendulum. *2015 IEEE International Conference on Control System, Computing and Engineering (ICCSCE)*, 218-223. IEEE.
3. Geylani, Ö. & Ata, B. (2026). Terminal and fast terminal sliding mode controls of a SISO coupled tank system: A comparative performance. *Çukurova Üniversitesi Mühendislik Fakültesi Dergisi, 41*(1), 75-88.
4. Zhang, J. & Zhang, H. (2012). LQR self-adjusting based control for the planar double inverted pendulum. *Physics Procedia, 24*, 1669-1676.
5. Sehgal, S. & Tiwari, S. (2012). LQR control for stabilizing triple link inverted pendulum system. *2012 2nd International Conference on Power, Control and Embedded Systems (ICPCES)*. IEEE.
6. Abdullah, A.I., Alnema, Y.H.S. & Thanoon, M.A. (2022). Stabilization of three links inverted pendulum with cart based on genetic LQR approach. *Journal Européen des Systèmes Automatisés, 55*(1), 125-130.
7. Önen, Ü., Çakan, A. & İlhan, İ. (2019). Performance comparison of optimization algorithms in LQR controller design for a nonlinear system. *Turkish Journal of Electrical Engineering and Computer Sciences, 27*(3), 1938-1953.
8. Bilgiç, H.H., Şen, M.A. & Kalyoncu, M. (2016). Tuning of LQR controller for an experimental inverted pendulum system based on The Bees Algorithm. *Journal of Vibroengineering, 18*(6), 3684-3694.

9. Ghoreishi, S.A. & Nekoui, M.A. (2012). Optimal weighting matrices design for LQR controller based on genetic algorithm and PSO. *Advanced Materials Research*, *433-440*, 7546-7553.

10. Xiong, X. & Wan, Z. (2010). The simulation of double inverted pendulum control based on particle swarm optimization LQR algorithm. *2010 IEEE International Conference on Software Engineering and Service Sciences*, 253-256. IEEE.

11. Shen, P. (2011). LQR control of double inverted-pendulum based on genetic algorithm. *2011 9th World Congress on Intelligent Control and Automation (WCICA)*, 386-389, IEEE.

12. Shen, P. (2014). Application of genetic algorithm optimization LQR weighting matrices control inverted pendulum. *Applied Mechanics and Materials, 543*, 1274-1277.

13. Abut, T. (2025). An inverted pendulum system control with fuzzy linear quadratic regulator method: Experimental validation. *Computers, Materials & Continua, 85*(2), 4023-4042.

14. Gen, M. & Lin, L. (2023). Genetic algorithms and their applications. In *Springer handbook of engineering statistics*, 635-674. London: Springer London.

15. Katoch, S., Chauhan, S.S. & Kumar, V. (2021). A review on genetic algorithm: past, present, and future. *Multimedia Tools and Applications*, *80*(5), 8091-8126.

16. Kennedy, J. & Eberhart, R. (1995). Particle swarm optimization. In *Proceedings of ICNN'95-international conference on neural networks, 4*, 1942-1948. IEEE.

17. Türksoy, Ö. (2026). A novel energy-efficient optimization framework for AVR controllers in modern power systems. *Çukurova Üniversitesi Mühendislik Fakültesi Dergisi*, *41*(2), 399-416.

18. Mirjalili, S., Mirjalili, S.M. & Lewis, A. (2014). Grey wolf optimizer. *Advances in Engineering Software*, *69*, 46-61.

19. Bel, M. ve Demir, H.G. (2025). Çift rotorlu MIMO sistemi için sürü zekâsı tabanlı LQGI kontrolcü tasarımı. *Erciyes Üniversitesi Fen Bilimleri Enstitüsü Fen Bilimleri Dergisi*, *41*(2), 631-646.

20. Mirjalili, S. & Lewis, A. (2016). The whale optimization algorithm. *Advances in Engineering Software*, *95*, 51-67.

21. Özcan, N., Utku, S. & Berber, T. (2025). Artificial circulation system algorithm: A novel bio-inspired algorithm. *Computer Modeling in Engineering & Sciences (CMES)*, *142*(1), 635-663.

22. Özcan, N. & Gürsoy-Demir, H. (2025). Levy flight-augmented artificial circulatory system algorithm for optimal PID tuning in DC motor control. *AEU-International Journal of Electronics and Communications*, 156101.